The 2013 World Congress on
Advances in Nano, Biomechanics, Robotics, and Energy Research (ANBRE13)
Seoul, Korea, August 25-28, 2013

The exergy loss distribution in subcritical organic Rankine cycle

Chao He, Chao Liu *, Xiao-Xiao Xu, Hong Gao and Hui Xie

Key Laboratory of Low-grade Energy Utilization Technologies and Systems of Ministry of Education, College of Power Engineering, Chongqing University, Chongqing 400030, China

Abstract: Taking net power output as optimization objective, the exergy loss distribution of subcritical ORC (organic Rankine cycle) system by using R245fa as the working fluid was calculated under the optimal conditions. The influences of heat source temperature, the evaporator pinch point temperature difference, the expander isentropic efficiency and the cooling water temperature rise on the exergy loss distribution of subcritical ORC system are comprehensively discussed. It is found that there exist a critical value of expander isentropic efficiency and cooling water temperature rise, respectively, under certain conditions. The magnitude of critical value will affect the relative distribution of exergy loss in the expander, the evaporator and the condenser. The research results will help to better understand the characteristics of the exergy loss distribution in an ORC system.

Keywords: subcritical Organic Rankine Cycle; exergy loss; expander isentropic efficiency

1. Introduction

With the fast growing of fossil fuel consumption, the use of low grade waste heat attracts public attention in recent years. Using low-grade waste heat not only can reduce fossil fuel consumption, but also can relieve the environmental problems. Organic Rankine Cycle is one of the attractive selections to recover low-grade waste heat. It has many advantages as compared with a traditional vapor Rankine cycle (Tamamoto et al. 2001; Liu et al. 2004; Wei et al. 2008; Roy et al. 2011).

Many investigations on ORC are mainly focused on the choices of the working fluid(Hung et al. 2010; Mago et al. 2007; Chen et al. 2010; Saleh et al., 2007; Lai et al. 2011) and its performance(Hung 2001; Wei et al. 2007; Mago et al. 2008; Tchanche et al. 2009; Aijundi 2011; Wang et al. 2011;Xu and He 2011; Guo et al. 2011a; Mago and Luck

*Corresponding author, Professor, E-mail address: liuchao@cqu.edu.cn.

2012). Hung (2001) discussed the irreversible loss of the key parts in ORC and found that the maximum irreversible loss happens in the evaporator. Analogously, Wei et al. (2007) showed the greatest irreversible loss occurs in the evaporator when waste heat temperature varies from 610K to 650K. Usually, the greatest exergy loss is in the evaporator under the given conditions (Mago et al. 2008; Tchanche et al. 2009; Aijundi 2011; Wang et al. 2011) and the smallest exergy loss is in the pump in ORC. But the magnitude of exergy loss in the expander and the condenser will change with different conditions such as expander isentropic efficiency and pinch point temperature difference.

The above research indicated that the exergy loss in the evaporator is the biggest, followed by the expander or condenser in subcritical ORC. Generally, these conclusions are obtained under given conditions which cannot wholly stand for real working conditions. The operation parameters in the real ORC are variable due to the change of the load and this will result in renewable irreversibility distribution in ORC. Some experimental research about the expander shows that the expander efficiency can vary from 30% to 85%(Manolakos et al. 2009; Peterson et al. 2008; Wang et al. 2010; Lemort et al. 2009; Quoilin et al. 2010; Li et al. 2011; Liu et al. 2010; James et al. 2009). To gain a better practical understanding about the irreversibility distribution in a subcritical ORC with low temperature heat source, it is necessary to study the irreversibility distribution under some different conditions.

2. System Description and Assumptions

Generally, the ORC system consists of a pump, an evaporator, an expander and a condenser, as shown in Fig.1.The working fluid is pumped from low pressure to high pressure, and then heated in the evaporator by waste heat to become a vapor with high pressure. The vapor enters into the expander to generate power. After work done in the expander, the high pressure vapor becomes a low pressure vapor and then it goes into the condenser where the low pressure vapor is condensed at a constant pressure to become a saturated liquid. Once the condensed saturated liquid returns back to the inlet of pump, another cycle of working fluid starts again. The corresponding ORC thermodynamic process on the T-S diagram is shown in Fig.2. The 3-4s and 1-2s in this figure are isentropic processes in the pump and the expander under ideal conditions, respectively.

There are three types of working fluid in the cycle: wet working fluid, isentropic working fluid and dry working fluid. We select isentropic fluid R245fa as the working fluid because of its good cycle performance(Mago et al. 2007; Chen et al. 2010) and eco-friendly characteristics(Guo et al. 2011b).

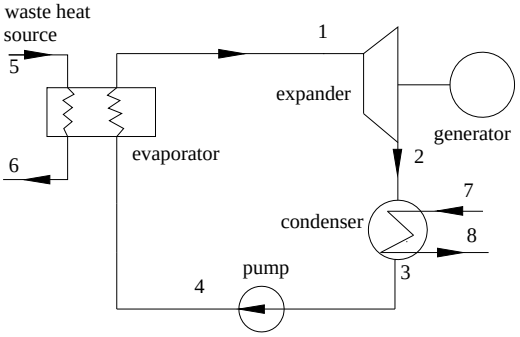

Fig.1. the system diagram of ORC

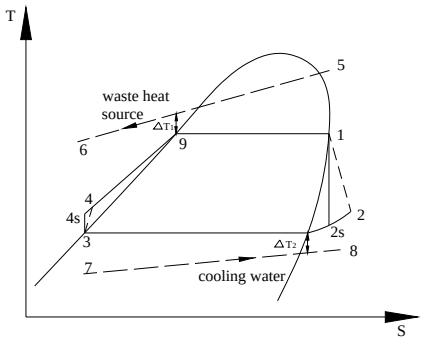

Fig.2. the T-s diagram of ORC

The simulation conditions are given in Table 1, and some other assumptions are made as follows: the system reaches a steady state; pressure drop in the evaporator, condenser and pipes, and heat losses between the whole system and the environment are negligible; the working fluid is at saturated liquid state at the outlet of condenser.

Table 1 Specifications of the ORC conditions

Description	Data
Waste heat inlet temperature(K)	373.15-433.15
The mass flow rate of heat source(kg/s)	1
The evaporator pinch point temperature difference (K)	5-20
Expander isentropic efficiency (%)	30-100
Pump isentropic efficiency (%)	75
Cooling water inlet temperature(K)	293.15
Cooling water temperature rise(K)	2-10
Environment temperature (K)	293.15
Environment pressure (kPa)	100

3. Mathematical Model

Based on the first and second laws of thermodynamics, the following equations could be obtained:

Process 4 to1: This is an isobaric heating process in the evaporator. The liquid working fluid absorbs heat from the low-grade waste heat source and becomes a saturated vapor. The total amount of heat transferred between the low-grade waste heat source and working fluid in the evaporator could be evaluated by the following equation:

$$\dot{Q}_{evp} = \dot{m}_h (h_5 - h_6) = \dot{m}_{wf} (h_1 - h_4) \quad (1)$$

The exergy loss in the evaporator:

$$\dot{I}_{evp} = T_0 \dot{m}_{wf} \left[(s_1 - s_4) - \frac{h_1 - h_4}{T_h} \right] \tag{2}$$

$$T_h = \frac{T_5 + T_6}{2} \tag{3}$$

where, h_5, h_6, h_4 and h_1 are the specific enthalpies of waste heat source and working fluid respectively; s_4 and s_1 are the working fluid specific entropies at the inlet and outlet of the evaporator; $\dot{m}_h$ and $\dot{m}_{wf}$ are the mass flow rate of heat source and working fluid; T_h, T_5, T_6, T_0 refer to the average temperature of waste heat source, the inlet and outlet temperature of waste heat source, the environment temperature, respectively.

Process 1 to 2: The high pressure vapor working fluid from the evaporator enters the expander, where the heat energy is converted into mechanical energy. The power is generated by the expander. For the ideal case, the process of 1-2s is an isentropic process. However, due to the irreversibility in the expander, the isentropic efficiency of expander is less than 100%. The power generated by the expander could be defined as:

$$\dot{W}_t = \dot{m}_{wf} (h_1 - h_2) = \dot{m}_{wf} (h_1 - h_{2s}) \eta_s \tag{4}$$

The exergy loss in the expander is as follows:

$$\dot{I}_t = T_0 \dot{m}_{wf} (s_2 - s_1) \tag{5}$$

where h_2 and h_{2s} refer to the specific enthalpies of working fluid in real and isentropic case at the outlet of expander, respectively; η_s is the expander isentropic efficiency.

Process 2 to 3: This is an isobaric heat rejection process in the condenser. The exhaust vapor at the outlet of the expander enters the condenser and releases the latent heat into the cooling water. The total heat released by the working fluid in the condenser could be expressed as:

$$\dot{Q}_c = \dot{m}_{wf} (h_2 - h_3) \tag{6}$$

The exergy loss in the condenser could be evaluated:

$$\dot{I}_c = T_0 \dot{m}_{wf} \left[(s_3 - s_2) - \frac{h_3 - h_2}{T_l} \right] \tag{7}$$

$$T_l = \frac{T_7 + T_8}{2} \tag{8}$$

where s_2 and s_3 are the specific entropies of the working fluid at the inlet and outlet of

condenser, respectively; h_2 and h_3 are the specific enthalpies of working fluid at the inlet and outlet of condenser; T_1, T_7, T_8 refer to the average temperature of cooling water, the cooling water temperature at the inlet and outlet of condenser, respectively.

Process 3 to 4: In the real situation, this is a non-isentropic compression process in the pump. The power input by the pump could be expressed as:

$$\dot{W}_p = \frac{\dot{m}_{wf}(h_{4s} - h_3)}{\eta_p} = \dot{m}_{wf}(h_4 - h_3) \tag{9}$$

The exergy loss in the pump could be evaluated:

$$\dot{I}_P = T_0 \dot{m}_{wf}(s_4 - s_3) \tag{10}$$

where, η_p is the isentropic efficiency of pump. h_{4s} refers to the specific enthalpy of working fluid in isentropic case at the outlet of pump. s_4 is the specific entropy of working fluid at the outlet of pump.

The net power output for the ORC could be given by:

$$\dot{W}_{net} = \dot{W}_t - \dot{W}_p \tag{11}$$

The first law efficiency of ORC system could be expressed as:

$$\eta_{th} = \frac{\dot{W}_{net}}{\dot{Q}_{evp}} \tag{12}$$

The second law efficiency or exergy efficiency of ORC system could be expressed as:

$$\eta_e^{sys} = \frac{\dot{W}_{net}}{\dot{E}_5} \tag{13}$$

where, E_5 is the exergy of the waste heat source at the inlet of the evaporator. It could be evaluated as follows:

$$\dot{E}_5 = \dot{m}_h \left[h_5 - h_0 - T_0(s_5 - s_0) \right] \tag{14}$$

where, h_5 and h_0 are the specific enthalpies of the waste heat source at the temperature of T_5 and T_0, respectively; T_0 is the environment temperature; s_5 and s_0 are the specific entropies of the waste heat source at temperature of T_5 and T_0, respectively.

The total exergy loss of the system could be expressed as follows:

$$\dot{I}_{tot} = \dot{I}_{evp} + \dot{I}_t + \dot{I}_c + \dot{I}_P \tag{15}$$

$$\dot{I}_{tot} = \dot{m}_{wf} T_0 \left[(-\frac{h_1 - h_4}{T_h}) - (\frac{h_3 - h_2}{T_l}) \right] \tag{16}$$

The proportion of exergy loss in the evaporator:

$$B_{evp} = \dot{I}_{evp} / \dot{I}_{tot} \tag{17}$$

The proportion of exergy loss in the expander:

$$B_t = \dot{I}_t / \dot{I}_{tot} \tag{18}$$

The proportion of exergy loss in the condenser:

$$B_c = \dot{I}_c / \dot{I}_{tot} \tag{19}$$

The proportion of exergy loss in the pump:

$$B_p = \dot{I}_p / \dot{I}_{tot} \tag{20}$$

The software EES (Engineering Equation Solver) is used to calculate thermal properties of working fluid and simulate the system performance. The quadratic approximations method is adopted to optimize the objective function. In the simulation process, the net output power is maximized by adjusting the evaporation temperature, and the exergy loss of ORC system is calculated when the net output power reaches the maximum value.

To verify the model, the simulation of subcritical ORC is carried out based on the assumptions provided by the reference (Dai et al. 2009). The optimized simulation results are shown in Table 2. From this table, it is evident that the results in this paper have good agreement with those in the reference(Dai et al. 2009). The differences between present paper and the reference are relatively small and these deviations could be explained by the different optimization method adopted in the simulations. The quadratic approximation method whose convergence error is 10^{-6} is adopted in this paper; however, a genetic algorithm whose convergence error is 10^{-4} is used in the reference (Dai et al. 2009).

Table 2 A comparison of results

Working fluid	T_1 (K)	P_1 (kPa)	T_2 (K)	P_2 (kPa)	T_4 (K)	$\dot{m}_{wf}$ (kg/s)	$\dot{W}_{net}$ (kW)	η_{th} (%)	Data source
R123	356.38	530	311.59	91	298.5	6.47	156.91	11.83	Ref.(Dai et al., 2009)
R123	356.4	531.7	312.2	91.48	298.5	6.036	147.9	11.88	This paper

4. Results and Analysis

4.1 The influence of heat source temperature and evaporator pinch point temperature difference

The relationships between the total exergy loss in ORC and heat source input temperature and the evaporator pinch point temperature differences are shown in Fig.3. Obviously the higher the heat source input temperature, the greater the total exergy loss of system. The influence of evaporator pinch point temperature difference on the total exergy loss is very small.

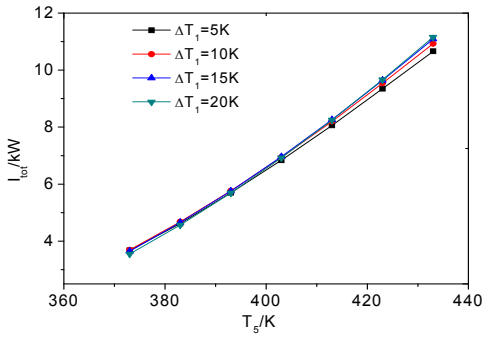

Fig.3. The change of the total exergy loss in ORC

When the isentropic efficiency of expander is 80% and the cooling water temperature rise is 5K, the proportion of exergy loss in the evaporator, expander, condenser and pump of ORC system are shown in Fig.4 with the different heat source input temperatures and evaporator pinch point temperature differences.

In Fig.4, at the same evaporator pinch point temperature difference, the proportion of exergy loss in the evaporator and condenser will reduce and those in the expander and pump will increase with the rise of heat source input temperature. However, at the same heat source input temperature, the proportion of exergy loss in the evaporator will increase and those in the expander, condenser and pump will reduce with the increase of evaporator pinch point temperature difference.

In order to conveniently compare the relationships between the proportion of exergy loss in the expander and condenser, the Fig.4(b) and Fig.4(c) could be combined in one figure, i.e., Fig.5. From this figure, it is clearly shown that a, b, c and d points are the four intersections of plotted curves when the evaporator pinch point temperature differences are 5K, 10K, 15K and 20K, respectively. On the left side of each point, the exergy loss in the condenser is greater than that in the expander, but on the right side of each point, the situation is opposite. With the increase of evaporator pinch point temperature difference,

the temperature of intersection point is more close to the high heat source input temperature.

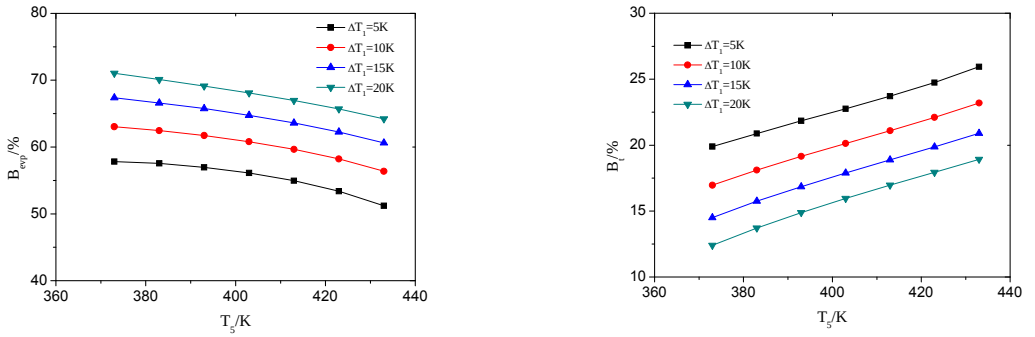

(a) evaporator (b) expander

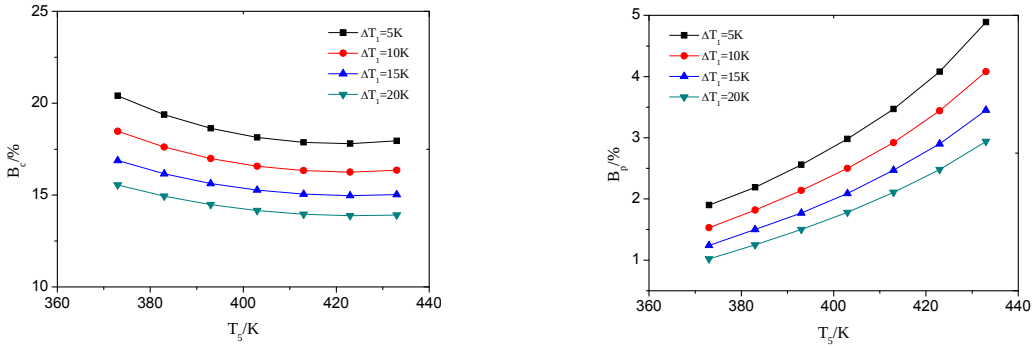

(c) condenser (d) pump

Fig. 4. The proportion of exergy loss in the evaporator, expander, condenser and pump of ORC

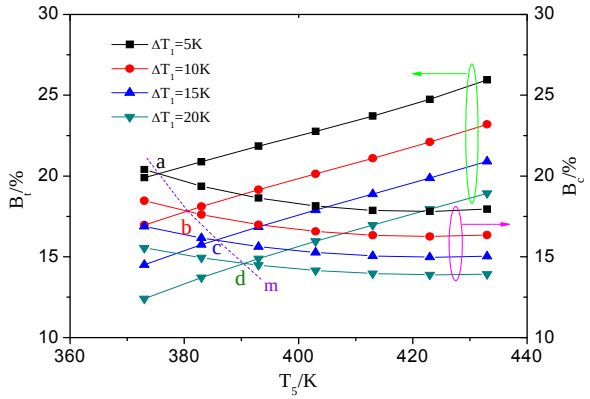

Fig. 5. The comparison of the proportion of exergy loss in the expander and condenser

4.2 The influence of expander isentropic efficiency

The total exergy loss in ORC at different expander isentropic efficiency is shown in Fig.6. Obviously, the higher the expander isentropic efficiency, the smaller the total exergy loss of system.

Fig.7 shows the relationship between the proportion of exergy loss in the evaporator and expander at different expander isentropic efficiency under the given conditions.

The proportions of exergy loss in the evaporator and expander are the same and the expander isentropic efficiency is about 40% for intersection point a in Fig.7(a). On the left side of point a, the exergy loss in the expander is greater than that in the evaporator, but on the right side of point a, the situation is opposite. When the evaporator pinch point temperature difference rises to 10K, the expander isentropic efficiency varies from 30% to 100% and there"s no intersection in the curves. This shows that the proportion of exergy loss in evaporator is always greater than that in expander.

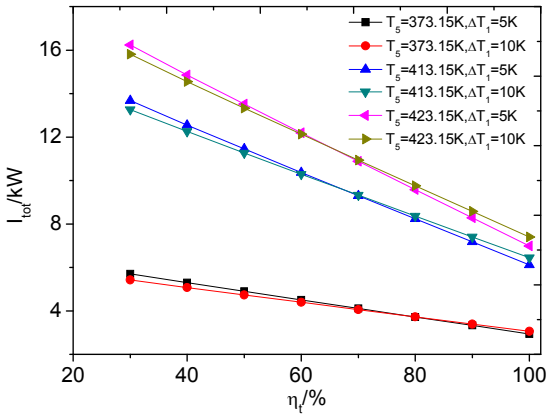

Fig.6. The total exergy loss in ORC at different expander isentropic efficiencies

When the heat source temperature is 413.15K, there are two intersection points a, b in the proportion of exergy loss curves for the evaporator and expander in Fig.7 (b) and Fig.7(c). The corresponding expander isentropic efficiency of point a is 41% and 52%, respectively; and that of point b is 45% and 55%, respectively. It can be seen that with the increase of heat source temperature, the corresponding expander isentropic efficiency will increase when the exergy losses in the evaporator and expander are the same.

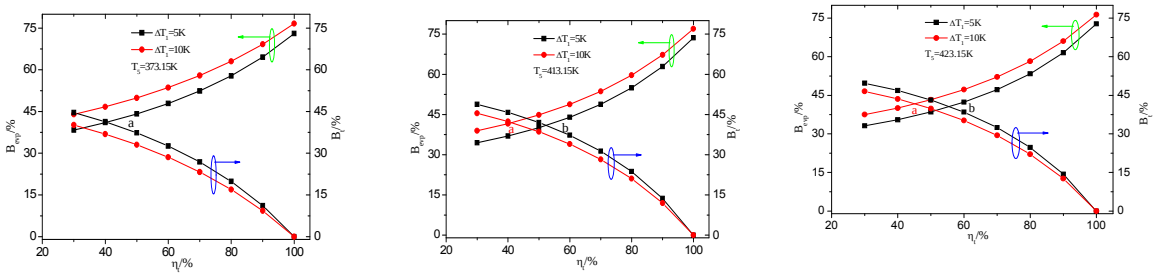

(a) (b) (c)

Fig.7. The influence of expander isentropic efficiency

Fig.8 shows the relationship between the proportion of exergy loss in the expander and condenser at different expander isentropic efficiencies. When the heat source temperature is 373.15K, there are two intersections a, b on the curves in Fig.8(a). The corresponding expander isentropic efficiency is about 80%.With the increase of expander isentropic efficiency, the exergy loss in the condenser is greater than that in the expander. When the heat source temperature goes up, Fig.8(b) and Fig.8(c) show a similar trend, and the corresponding expander isentropic efficiency of points a and b is about 85% .

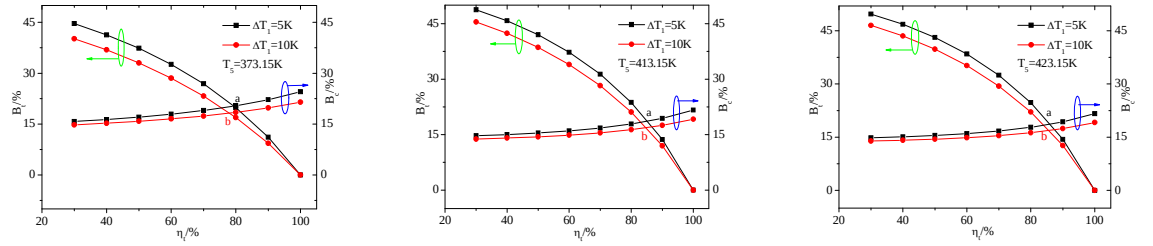

(a) (b) (c)

Fig.8. The influence of expander isentropic efficiency

The change of the heat source temperature and the expander isentropic efficiency will result in the change of the proportion of exergy loss in the condenser and expander. During the running periods of ORC, many factors will affect the working conditions of ORC and cause change of the proportion of exergy loss in ORC. This question should be worth paying attention.

4.3 The influence of cooling water temperature rise

When the isentropic efficiency of expander is 80%, the relationships between the total exergy loss in ORC, the heat source input temperature and the cooling water

temperature rise are shown in Fig.9. Obviously, the total exergy loss of system gets reduced with the increase of cooling water temperature rise.

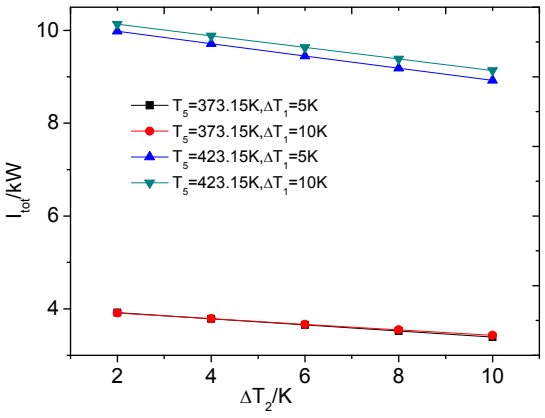

Fig.9. The total exergy loss versus cooling water temperature rise

Fig.10 shows the relationship between the proportion of exergy loss in the expander and condenser with different cooling water temperature rise. There are two intersections (i.e., points a and b) in the curves in Fig.10(a). The corresponding cooling water temperature rise for points a and b is about 5K and 6K, respectively. It can be seen that the change of cooling water temperature rise will also affect the proportion of exergy loss in the expander and condenser. The exergy loss in the expander is always greater than that in the condenser in the range of studied cooling water temperature rise in Fig.10(b).

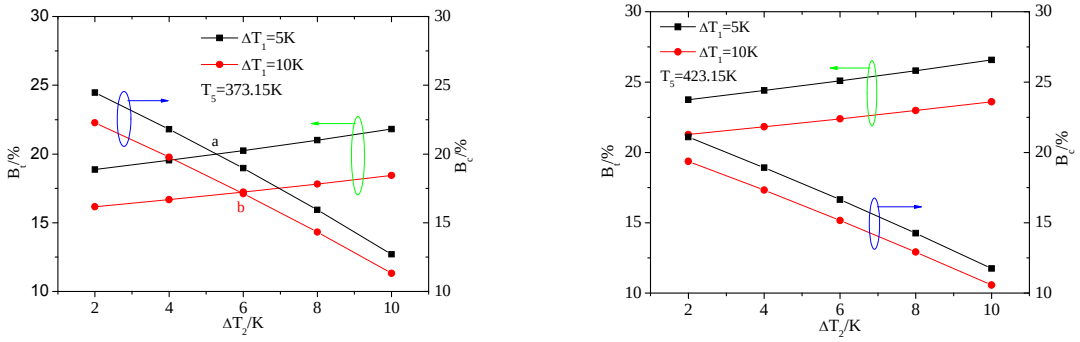

(a) (b)

Fig.10. The influence of cooling water temperature rise

5. Conclusions

This paper discussed the influence of heat source temperature, the evaporator pinch point temperature difference, the expander isentropic efficiency and the cooling water temperature rise on the exergy loss distribution of subcritical ORC system by using R245fa as the working fluid. The main conclusions can be summarized as follows:

The total exergy loss in ORC will increase with the rise of the heat source input temperature and will reduce with the increase of the expander isentropic efficiency. The magnitude of evaporator pinch point temperature difference almost does not affect the total exergy loss in ORC. The greater cooling water temperature rise will help to reduce the total exergy loss in ORC.

Under a certain condition of the heat source temperature and the evaporator pinch point temperature difference, there exists a critical value of the expander isentropic efficiency. When the expander isentropic efficiency is smaller than the critical value, the exergy loss in the expander will be greater than that in the evaporator. For the condenser and expander, there also exists a critical value of the expander isentropic efficiency. The exergy loss in the condenser may exceed that in the expander. There exists a critical value of the cooling water temperature rise. When the cooling water temperature rise is higher than this critical value, the exergy loss in the expander will be greater than that in the condenser.

Acknowledgments

This work was supported by National Basic Research Program of China (973 Program) under Grant No. 2011CB710701.

References

Aijundi, I.H. (2011), “Effect of dry hydrocarbons and critical point temperature on the efficiencies of organic Rankine cycle”, *Renew. Energy*, Vol.**36**, 1196–1202.

Chen, H.J., Goswami, D.Y. and Stefanakos, E.K. (2010), “A review of thermodynamic cycles and working fluids for the conversion of low-grade heat”, *Renew. Sustain. Energy*, Vol.**14**, 3059–3067.

Dai, Y.P., Wang, J.F. and Lin, G. (2009), “Parametric optimization and comparative study of organic Rankine cycle (ORC) for low grade waste heat recovery”, *Energy Convers. Manage.*, Vol.**50**, 576–582.

Guo, T., Wang, H.X. and Zhang, S.J. (2011a), “Comparative analysis of natural and conventional working fluids for use in transcritical Rankine cycle using low-temperature geothermal source”, *International Journal of Energy Research*, Vol.**35**, 530-544.

Guo, T., Wang, H.X. and Zhang, S.J. (2011b), “Fluids and parameters optimization for a novel

cogeneration system driven by low-temperature geothermal sources", *Energy*, Vol.**36**, 2639–2649.

Hung, T.C. (2001), "Waste heat recovery of organic Rankine cycle using dry fluids", *Energy Convers. Manage.*, Vol.**42**, 539–553.

Hung, T.C., Wang, S.K., Kuo, C.H., Pei, B.S. and Tsai, K.F. (2010), "A study of organic working fluids on system efficiency of an ORC using low-grad energy sources", *Energy*, Vol.**35**, 1403-1411.

James, A.M., Jon, R.J., Cao, J., Douglas, K.P. and Richard, N.C. (2009), "Experimental testing of gerotor and scroll expanders used in, and energetic and exergetic modeling of an organic Rankine cycle", *J. Energy Resour. Technol.*, Vol.**131**, 201–208.

Lai, N.A., Wendland, M. and Fischer, J. (2011), "Working fluids for high- temperature organic Rankine cycles", *Energy*, Vol.**36**, 199–211.

Lemort, V., Quoilin, S., Cuevas, C. and Lebrun, J. (2009), "Testing and modeling a scroll expander integrated into an organic Rankine cycle", *Appl. Therm. Eng.*, Vol.**29**, 3094–3102.

Liu, G., Zhao, Y., Li, L. and Shu, P. (2010), "Simulation and experiment research on wide ranging working process of scroll expander driven by compressed air", *Appl. Therm. Eng.*, Vol.**30**, 2073–2079.

Li, J., Pei, G., Li,Y.Z. and Ji, J. (2011), "Evaluation of external heat loss from a small-scale expander used in organic Rankine cycle", *Appl. Therm. Eng.*, Vol.**31**, 2694–2701.

Liu, B.T., Chien, K.H. and Wang, C.C. (2004), "Effect of working fluids on organic Rankine cycle for waste heat recovery", *Energy*, Vol. **29**, 1207–1217.

Manolakos, D., Kosmadakis, G., Kyritsis, S. and Papadakis, G. (2009), "Identification of behaviour and evaluation of performance of small scale, low-temperature organic Rankine cycle system coupled with a RO desalination unit", *Energy*, Vol.**34**, 767–774.

Mago, P.J., Chamra, L.M. and Somayaji, C. (2007), "Performance analysis of different working fluids for use in organic Rankin cycles", *Proc. I.M.E. J. Power Energ.*, Vol.**221**, 255–264.

Mago, P.J., Srinivasan, K.K., Chamra, L.M. and Somayaji, C. (2008), "An examination of exergy destruction in organic Rankine cycles", *Int. J. Energ. Res.*, Vol.**32**, 926–938.

Mago, P.J. and Luck, R. (2012), "Energetic and exergetic analysis of waste heat recovery from a microturbine using organic Rankine cycles", *Int. J. Energ. Res.*, doi: 10.1002/er.2891.

Peterson, R.B., Wang, H. and Herron, T. (2008), "Performance of small-scale regenerative Rankine power cycle employing a scroll expander", *Proc. IME. J. Power Energ.*, Vol.**222**, 271–282.

Quoilin, S., Lemort, V. and Lebrun, J. (2010), "Experimental study and modeling of an organic Rankine cycle using scroll expander", *Appl. Energy*, Vol.**87**, 1260–1268.

Roy, J.P., Mishra, M.K. and Misra, A. (2011), "Performance analysis of an Organic Rankine Cycle with superheating under different heat source temperature conditions", *Appl. Energy*, Vol.**88**, 2995-3004.

Saleh, B., Koglbauer, G., Wendland, M. and Fischer, J. (2007), “Working fluids for low-temperature organic Rankine cycles”, *Energy*, Vol.**32**, 1210–1221.

Tamamoto, T., Furuhata, T., Arai, N. and Mori, K. (2001), “Design and testing of the organic Rankine cycle”, *Energy*, Vol.**26**, 239–251.

Tchanche, B.F., Papadakis, G., Lambrinos, G. and Frangoudakis, A. (2009), “Fluid selection for a low-temperature solar organic Rankine cycle”, *Appl. Therm. Eng.*, Vol.**29**, 2468–2476.

Wang, E.H., Zhang, H.G., Fan, B.Y., Ouyang, M.G., Zhao, Y. and Mu, Q.H. (2011), “Study of working fluid selection of organic Rankine cycle (ORC) for engine waste heat recovery”, *Energy*, Vol.**36**, 3406–3418.

Wang, X.D., Zhao, L., Wang, J.L., Zhang, W.Z., Zhao, X.Z. and Wu, W. (2010), “Performance evaluation of a low-temperature solar Rankine cycle system utilizing R245fa”, *Sol. Energy*, Vol.**84**, 353–364.

Wei, D.H., Lu, X.S., Lu, Z. and Gu, J.M. (2007), “Performance analysis and optimization of organic Rankine cycle (ORC) for waste heat recovery”, *Energy Convers. Manage.*, Vol.**48**, 1113–1119.

Wei, D.H., Lu, X.S., Lu, Z. and Gu, J.M. (2008), “Dynamic modeling and simulation of an Organic Rankine Cycle(ORC) system for waste heat recovery”, *Appl. Therm. Eng.*, Vol.**28**, 1216–1224.

Xu, R.J. and He, Y.L. (2011), “A vapor injector-based novel regenerative organic Rankine cycle”, *Appl. Therm. Eng.*, Vol.**31**, 1238–1243.

Nomenclature

B the proportion of exergy loss

$\dot{E}$ exergy(kW)

h specific enthalpy(kJ kg^{-1})

$\dot{I}$ exergy loss(kW)

$\dot{m}$ mass flow rate (kg s^{-1})

$\dot{Q}$ the heat rate injected and rejected(kW)

s specific entropy (kJ kg^{-1})

T temperature (K)

T_h the average temperature of waste heat source (K)

T_l the average temperature of cooling water (K)

$\dot{W}$ power output or input (kW)

Greek symbols

η efficiency (dimensionless)

Subscripts

c condenser

evp evaporator

g generator

h	waste heat source
net	net
p	pump
s	isentropic
t	expander
th	thermal
tot	total
wf	working fluid
0	reference state point
1-8	state points
2s,4s	stat points for the ideal case